BOUNDARY ELEMENT MODELING OF THE RAHE DORSUM THRUST FAULT ON ASTEROID 433 EROS.

T. R. Watters[1] and **M. S. Robinson**[2], [1]Center for Earth and Planetary Studies, National Air and Space Museum, Smithsonian Institution, Washington, D.C. 20560 (twatters@nasm.si.edu); [2]Department of Geological Sciences, Northwestern University, Evanston, Illinois 60208 (robinson@eros.earth.nwu.edu).

Introduction: Rahe Dorsum is one of the most striking features on the surface of Eros. It generally has tens of meters of relief and extends for about 18 km (Fig. 1) making it a global-scale feature [1, 2]. Rahe Dorsum appears to be a series of segments that are generally asymmetric in crosssection [1, 2]. Rahe Dorsum strongly resembles landforms called lobate scarps found on Mercury, Mars, and the Moon [see 3, 4].

Topography: NEAR Laser Altimeter (NLR) data has provided unprecedented detail of the topography of an asteroid [5, 6]. A total of almost 16 million measurements from the spacecraft to the asteroid were made. The single shot precision of the measurements are about 1 m at 40 km range [7]. An NLR profile across Rahe Dorsum shows that it is analogous to planetary lobate scarps (Fig. 1, 2).

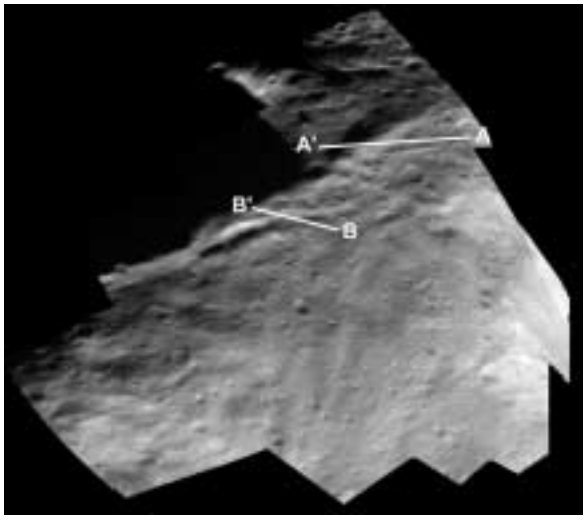

Figure 1. MSI mosaic of Rahe Dorsum near Tutanekai crater. The locations of two NLR profiles that cross the ridge are indicated (see Figure 2 and 3). The mosaic shows the presence of a smaller subsidiary ridge flanking Rahe Dorsum (see Figure 3).

The lengths of profiles were determined by projecting their trace onto a sphere with the radius defined by the average radius along the profile. Located roughly midway along the structure (east of Tutanekai crater), Rahe Dorsum has a maximum relief of ~130 m where the profile crosses the structure. The image and topographic data reveals the existence of a smaller subsidiary ridge flanking Rahe Dorsum (Fig. 1).

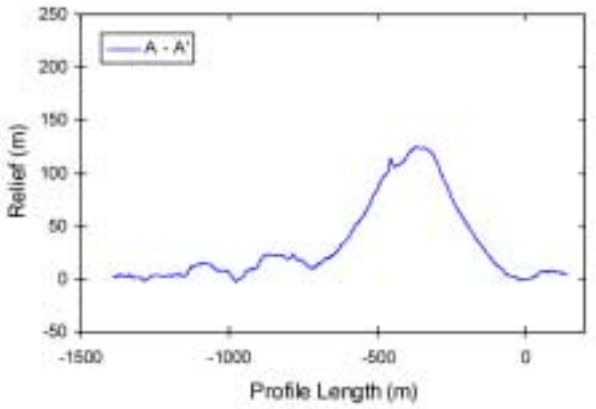

Figure 2. Topographic profile across Rahe Dorsum. The profile was generated by subtracting the NLR radius from an equipotential surface. The elevations are then detrended to an arbitrary datum. Profile location is shown in Figure 1. Vertical exaggeration is ~4X.

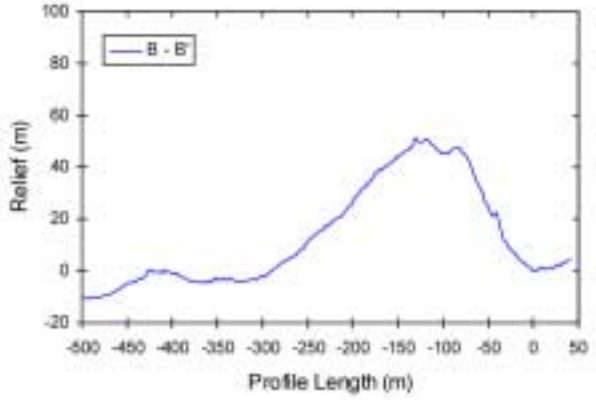

Figure 3. Topographic profile across a subsidiary ridge flanking Rahe Dorsum. The profile was generated by subtracting the NLR radius from an equipotential surface. The elevations are then detrended to an arbitrary datum. Profile location is shown in Figure 1. Vertical exaggeration is ~3X.

This ridge has a maximum relief of about 50 m where the profile crosses it (Fig. 3).

Boundary Element Modeling: The displacement and stresses above a propagating fault can be modeled using the boundary elements [8, 9]. For thrust faults, the fault surface is defined as a rectangular plane having a fault-plane dip θ, and vertical depth of faulting T (Fig. 4) [10, 11]. It is assumed that deformation has occurred above a blind thrust fault. Forward mechanical modeling of Rahe Dorsum

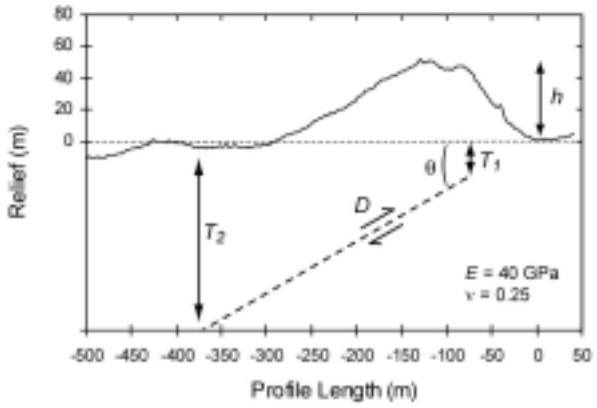

Figure 4. Model parameters shown with the topographic profile across the secondary ridge associated with Rahe Dorsum. The underlying thrust fault has an upper and lower depth of faulting T_1 and T_2, fault-plane dip angle θ, and maximum displacement D. The depth of faulting is not to scale. Vertical exaggeration of topography is ~2X.

constrained by the topographic data suggests the underlying fault has a fault-plane dip of ~40°, a maximum depth of faulting of ~500 m, and a displacement of ~175 m (Fig. 5). The modeling also demonstrates that a planar fault geometry produces a

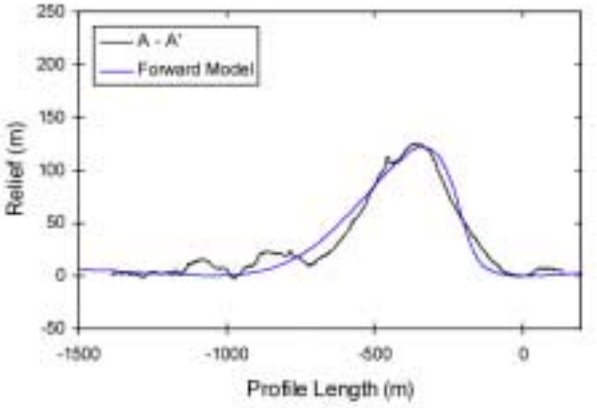

Figure 5. Comparison of predicted structural relief and topography across Rahe Dorsum. The model shown is for a fault-plane dip θ of 40°, a maximum depth of faulting T_2 of 500 m, and a displacement D of 175 m. Profile location is shown in Figure 1. Vertical exaggeration is ~4X.

good match to the cross-sectional topography of the ridge. The fit does not improve by changing the geometry to a listric shape [see 11]. Modeling of the secondary ridge suggests an underlying fault with a dip of ~35°, a maximum depth of faulting of ~200 m, and a displacement of ~80 m (Fig. 6).

Implications: The widespread occurrence of grooves and troughs on Eros has been interpreted as evidence of a pervasive fabric of fractures induced by impacts and collisions [1]. An analysis of the ridges, troughs and grooves on Eros indicate that only two features align over a large fraction of the asteroid's length, Rahe Dorsum and Calisto Fossae, a degraded set of parallel troughs interpreted to be the result of extension [2, 13]. The degraded appearance of Calisto Fossae and the large number of superimposed craters suggests that it is much older than Rahe Dorsum [14]. Planes fit to Rahe Dorsum and Calisto Fossae indicate that they are generally coplanar, and the plane defined by the two structures is roughly parallel to a surface facet of Eros [14]. It has been suggested that both compressional and extensional features were

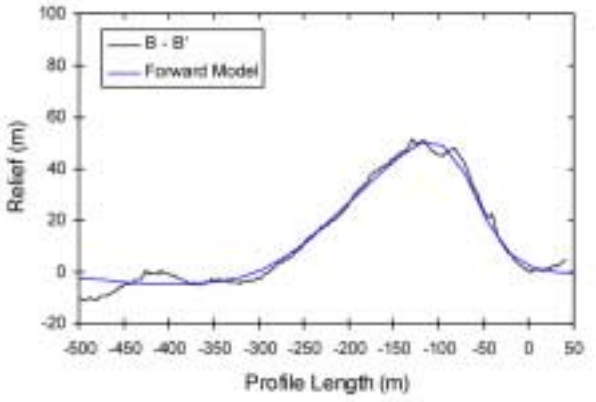

Figure 6. Comparison of predicted structural relief and topography across the secondary ridge flanking Rahe Dorsum. The model shown is for a fault-plane dip θ of 35°, a maximum depth of faulting T_2 of 200 m, and a displacement D of 80 m. Profile location is shown in Figure 1. Vertical exaggeration is ~3X.

influenced by a nearly global, pervasive fabric of fractures and joints [14], and that the fault underlying Rahe Dorsum exploited this preexisting fabric [1, 2].

Our results suggest Rahe Dorsum and its subsidiary ridge are the surface expressions of shallow-rooted thrust faults. These thrust faults do not appear to have been influenced by reactivation of a preexisting fracture system controlling the location of Calisto Fossae. The source of the compressional stresses that formed the thrust faults is being investigated.

References: [1] Veverka J. et al. (2000) *Science, 289*, 2088-2097. [2] Prockter L. et al. (2002) *Icarus, 155*, 75-93. [3] Watters T.R. (2003) *JGR*, in press. [4] Watters T.R., Robinson M.S. and Cook A.C. (2001) *Planet. Space Sci. 49 (14-15)*, 1523-1530. [5] Zuber M.T. et al. (1997) *JGR, 102*, 23761-23773. [6] Zuber M.T. et al. (2000) *Science, 289*, 2097-2101. [7] Cheng A.F. et al. (2002) *Icarus, 155*, 51-74. [8] King G.C.P., Stein R.S. and Lin J. (1994) *Bull. Seism. Soc. Am., 84*, 935-953. [9] Toda S. et al. (1998) *JGR, 103*, 24543-24565. [10] Schultz R.A. and Watters T.R. (2001) *GRL, 28* , 4659-4662. [11] Watters T.R., Schultz R.A., Robinson M.S. and Cook A.C. (2002) *GRL, 28*, 4659-4462. [12] Watters T.R. and Schultz R.A. (2002) *LPSC XXXIII*, 1668. [13] Thomas P.C. et al. (2002) *Icarus, 155*, 18-37. [14] Thomas P.C. et al. (2002) *GRL, 29*, 46-1—46-4.